Proceedings of the 21st ICSMGE, Vienna, Austria, 14 – 19 June 2026. Pistrol, Adam & Schweiger (eds.)
Published by: ÖGG, Austrian Society for Geomechanics, Salzburg, Austria, ISBN 978-3-9503898-4-5
https://doi.org/10.53243/ICSMGE2026-1118

Smart quay walls: case study Amaliahaven

Chris van Marrewijk, Jan Putteman
SBE Nederland BV, the Netherlands, chris.vanmarrewijk@sbe-engineering.nl

Joris Bruens, Joppe Burgers
Port of Rotterdam, the Netherlands

Alfred Roubos
Port of Rotterdam, the Netherlands
Delft University of Technology, the Netherlands

ABSTRACT: In the coming years, approximately half of the quay walls in Rotterdam will reach the end of their design lifetime. Uncertainties in quay-wall modelling make it difficult to determine their exact technical end-of-life. To gain insight into the actual performance, the Port Authority has equipped new quay walls with sensors. This paper evaluates the sensors installed in the Amaliahaven quay wall and compares field observations with predictions from design models. The project involves the development of a 1.8 km deep-sea quay wall with a soil-retaining height of 29 meters. The superstructure includes an 18.5-meter-wide relieving platform, while the substructure consists of a combined wall and driven cast-in-situ piles. The quay wall is anchored with screw injection anchors. For the critical measurement locations, appropriate sensors were selected. Five open-ended tubular piles and ten driven cast-in-situ piles are equipped with fiber optic strain sensors and inclinometer casings to measure bending moments, axial forces and deformations along the pile length. Forces along the full length of twenty-two ground anchors are measured with fiber optic strain sensors, while the force of eight anchors is also measured using load cells. Additional sensors tracking water levels, tilt, displacement, and mooring loads make this quay wall globally unique. During construction, sensors underwent rigorous testing to ensure accuracy. Smart piles were subjected to bending tests, and ground anchors were tested to match measured and applied forces. Soil pressure is the governing load acting on a soil-retaining quay wall. During dredging, the strains begin to accumulate and stabilize post-dredging. This paper shows the potential of monitoring data for understanding the quay wall's behavior and updating of computational models, as in the coming years a lot of monitoring data will be collected for a range of boundary conditions, such as tidal effects, temperature/seasonal changes, mooring loads and crane loads.

KEYWORDS: quay wall, structural health monitoring, fiber optic sensor.

1 INTRODUCTION

Container volumes in Rotterdam (the Netherlands) are expected to continue to grow strongly in the coming years. For this reason the Port of Rotterdam Authority invests in the further expansion of the Prinses Amaliahaven quay walls located on Maasvlakte II. The project involves the construction of:

- 1,825 meters of deep-sea quay wall, with a soil retaining height of 29 meters.
- 1,825 meters of back crane track with pile foundation
- 160 meters of inland shipping quay wall

Construction works ended in 2025. A large amount of foundation elements have been installed (together, these are referred to as the 'substructure' of the quay wall):

- ca. 700 open-ended tubular piles and intermediate sheet piles (combined wall)
- ca. 2100 driven cast-in-situ piles
- ca. 1300 screw injection (SI) anchors

The Port of Rotterdam Authority decided to invest in monitoring of the quay wall, primarily for the reasons below:

- In the coming years, approximately half of the quay walls in Rotterdam will reach the end of their design lifetime. Uncertainties in quay-wall modeling make it difficult to determine their exact technical end-of-life.
- The perception that the design of quay walls incorporate implicit safety margins and conservative assumptions, which do not necessarily enhance reliability, yet impede material efficiency and sustainability.

Based on the monitoring data, the design models (including Plaxis2D) can be updated through reverse engineering, which in turn results in an update of the technical requirements of the quay wall. It is expected that, in the future, customer value and return on investment can be achieved by allowing a higher surcharge load, a larger vessel type, or by extending the service life of the quay wall based on structural health monitoring data. Furthermore, new insights might lead to more optimized design methods for future, similar projects.
The focus of the monitoring is on the substructure, as the uncertainties and knowledge gaps in geotechnics and soil-structure interaction are much greater than in the structural engineering of steel and concrete.

2 MONITORING DESIGN

A general overview of the cross-section of the deep-sea quay wall is provided in Figure 1 including all structural elements. The Amaliahaven quay wall is equipped with sensors on different structural elements for both the sub- and superstructure (relieving platform).

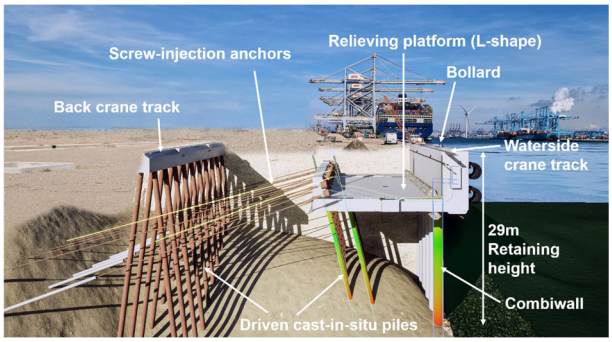

Figure 1. Cross-section of deep-sea quay wall at Amaliahaven.

The aim of the monitoring equipment is to measure strains, forces and deformations. Furthermore, several boundary

conditions are measured such as the temperature and (ground)water levels. A global overview of all sensors is given below for each structural element, including a short elaboration on why and how these sensors are applied. For the fiber optic sensors, load cells, tiltmeters and piezometers, the measurement frequency is once every 30 minutes.

2.1 *General*

Most of the monitoring applied at Amaliahaven is relatively straightforward and therefore not discussed in detail. This includes inclinometer measurements, piezometers, tiltmeters, etc. In contrast, fiber optic sensors require more attention in both installation and data analysis. As a result, this paper focuses primarily on these sensors. A significant number of Brillouin distributed sensors (BOFDA double ended measurements) have been deployed, measuring both strain and temperature throughout the total fiber length. The optical fibers, supplied by fibrisTerre, are connected to the fTB 5020 interrogator. Temperature compensation is essential in fiber optic strain sensing since both strain and temperature affect the optical signal. Without compensation, it's impossible to distinguish whether a change in the signal is due to mechanical strain or thermal expansion/contraction. Temperature fluctuations (day/night cycles, seasonal changes) can introduce false strain readings if not compensated. Hence, for every fiber optic sensor fixed to the structure, a parallel reference fiber is provided right next to it. The latter is not bonded to the structure and only responds to temperature.

In general, the following steps must be executed in order to retrieve the desired physical quantities for all fiber optic sensors.

1. Determine the relative strain

The absolute strain must be related to the reference measurement (no-load condition). The reference measurement is performed before the dredging phase of the quay wall, which exerts the highest loads on the structure.

2. Determine the mechanical strain

The relative strains as determined in step 1 must be corrected for temperature effects with $\Delta\varepsilon_T$ according to the following formula:

$$\Delta\varepsilon_T = \frac{\Delta\varepsilon \cdot (\alpha_{T,Fiber\ Optic} + \alpha_{T,Steel})}{\alpha_{T,Fiber\ Optic}} \quad (1)$$

Where $\Delta\varepsilon_T$ represents the temperature-induced strain to correct for, $\Delta\varepsilon$ represents the change in strain for the temperature fiber optic sensor, $\alpha_{T,Steel}$ is the thermal expansion coefficient of steel (ca. 12 * 10^{-6}/°C) and $\alpha_{T,Fiber\ Optic}$ is the temperature coefficient to account for the change of the refraction index (ca. 7.32 *10^{-6}/°C)

3. Determine the mechanical strain at the outer edge of the pile by correcting for the geometrical position of the sensor.
4. Determine the mechanical stress with the E-modulus of the material, i.e. concrete/steel.
5. Determine the desired physical quantities with the cross-sectional properties of the element (I_x, W_x, A).

An overview of the total monitoring package is summarized below in Table 1. The axial force is represented by N, the bending moment by M_i and the deformation by U_i. The subscript 'i' shows the direction, generally perpendicular and parallel to the quay wall.

2.2 *Substructure*

The substructure is most critical within the modelling of soil-structure interaction. This is a domain where large uncertainties lie in (geotechnical) modelling. Hence, the substructure is equipped with an extensive package of monitoring.

Table 1: Overview monitoring Amaliahaven quay wall

Element	#	Monitoring	Output
Tubular Pile	5	Distributed fiber optic sensors (4x/pile)	N, M_Y
	20	Inclino measurements	U_X, U_Y
Driven cast-in-situ pile	10	Distributed fiber optic sensors (4x/pile)	N, M_Y, M_Z
	10	Inclino measurements	U_X, U_Y
SI Anchors	22	Distributed fiber optic sensors (1x)	N
	8	Load cells	N (at head)
Relieving platform	80	Survey bolts	U_X, U_Y, U_Z
	5	Tiltmeter	i_X, i_Y
Bollards	108	Mooring load measurement	$F_{BOLLARD}$
Groundwater/ Harbour level	20 4	Piezometers	h_{GWL} h_{WL}
Leakage-induced settlement	1	Distributed fiber optic sensor (along 1825 m)	-

2.2.1 *Tubular piles*

The tubular piles are equipped with inclinometer casings. The inclinometer measures the horizontal deformations of the tubular pile. Besides, the deformation can be converted to the local curvature of the tubular pile. In turn, the curvature can be correlated to the bending moment line with the relation $M = EI \cdot \kappa$, where κ is equal to the 2nd derivative of the deformation U over the pile length L; $\kappa = \frac{\delta^2 U}{\delta L^2}$.

Secondly, the tubular piles are equipped with fiber optic sensors. Each pile is provided with four fiber optic sensors; two on the landside and two on the waterside as indicated in Figure 2. Two fiber optic sensor lines are glued to the pile before pile driving, and two fiber optic sensor lines are inserted into a steel casing and fixed with a grout mixture after pile driving.

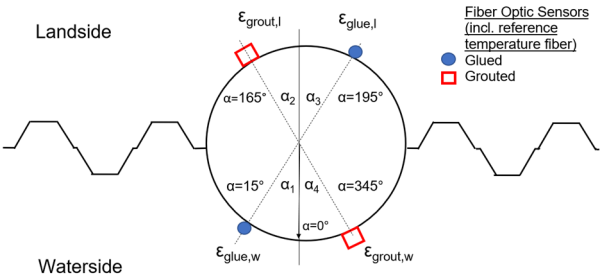

Figure 2. Cross-section of tubular pile including fiber optic sensors.

Ultimately, the axial force N and the bending moment M_y can be determined according to §2.1. Finally, these structural forces can be directly compared to the design models.

2.2.2 *Screw injection anchors*

The screw injection (SI) anchors provide horizontal anchorage of the deep-sea quay wall and are subject to very high tensile loads. As a grouted anchor, it is prone to execution-related variability. Furthermore, the couplers between the anchor rod elements are critical components. Due to its shallow inclination, the ground anchor is susceptible to increased tensile stress resulting from soil settlement. For these reasons, the SI anchors are most numerously monitored in this project. The SI anchors are equipped with fiber optic sensors, where the sensors are installed in the hollow part of the anchor rod and finished with grout. As the sensor is located on the neutral axis of the anchor rod, only axial strains are measured for the anchors resulting in axial forces N only.

Eight of these anchors have an additional load cell at the top of the anchor as a separate redundant anchor monitoring system.

2.2.3 *Driven cast-in-situ piles*

The driven cast-in-situ piles are known to be a critical part of a deep-sea quay wall with a relieving platform. It must withstand both large axial forces and bending moments. The inclinometer casings serve the same goal as for the tubular piles. Moreover, each driven cast-in-situ pile is provided with 4 fiber optic sensors. The fiber optics are equally distributed over the cross-section with 90° offset angle. As the rotation angle of the rebar cage depends on installation, it is important to measure the rotation angle of each rebar cage on site after installation. Subsequently, the structural forces N, M_y and M_z can be derived according to the principle shown in §2.1. As the sensors are equally distributed over the cross-section with 90° offset angle, bi-directional bending effects can be captured with sufficient accuracy (contrary to the tubular piles which only allow for accurate one-directional bending measurement). The fiber optic sensors are fixed to the inside of the reinforcement cage of the pile with cable ties. The fiber optic sensors and the inclinometer casing are shown in Figure 3.

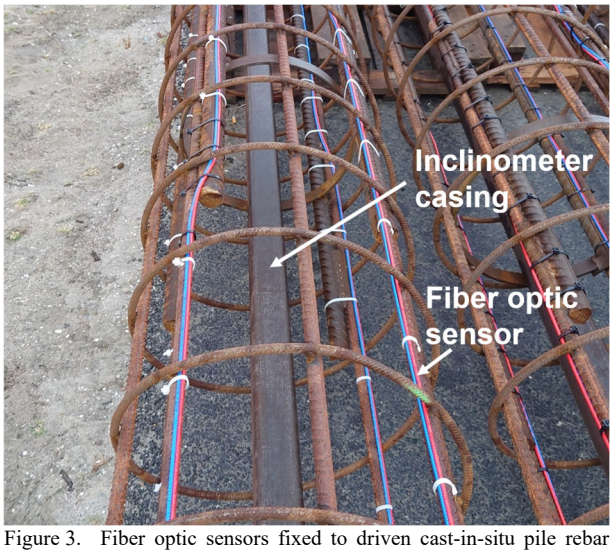

Figure 3. Fiber optic sensors fixed to driven cast-in-situ pile rebar cage and inclinometer casing

2.3 *Superstructure*

The superstructure is less critical within the modelling of soil-structure interaction. The connection between the relieving platform and the tubular pile is constructed with a cast steel 'saddle', which is a typical solution in the Port of Rotterdam and functions as a hinge. Combined with the support at the driven cast-in-situ piles, the relieving platform can be interpreted as a quasi-statically determinate system. Hence, the deformations of the soil/substructure do not result in large differences in the internal forces of the superstructure. To conclude, the uncertainties within the modelling of the soil-structure interaction do not affect the superstructure significantly. This explains why the provided monitoring package of the superstructure is less extended compared to the substructure.

2.3.1 *Relieving platform*

The focus within the monitoring of the relieving platform lies within its deformations. First of all, each section of the relieving platform (with a width of ca. 23 m) has four survey bolts. Two bolts on each joint are installed on top of the front wall. These bolts are fixed points where the coordinates are manually measured with a total station, resulting in the deformations or movement of the relieving platform. This applies to all 80 sections of the Amaliahaven. Secondly, five sections are equipped with tilt sensors as well. They measure the inclination of the front wall. As a result, the information provided by both the survey bolts and the tilt sensors result in the translation and bi-directional rotation of the superstructure.

2.4 *Boundary conditions and others*

The load exerted on the quay wall by bollards is significant, with a design capacity equal to 300t per bollard and 2 bollards per 15m of quay wall. The actual bollard load is a major boundary condition driving the anchor force. As the bollard fixes the vessel to the quay wall, the bollard load depends on wind conditions, vessel dimensions, mooring configuration, etc. Without accurate measurements, the interpretation of the anchor force would be very difficult. For this reason, the part of the quay wall most exposed to storm conditions was fully equipped with smart bollards. As a patented system from a Dutch supplier was used, the functioning of the smart bollard is not further elaborated upon in this paper.

As mentioned in Table 1, both groundwater level and harbour water level are being measured.

3 SITE ACCEPTANCE TESTS

In previous projects involving deep-sea quay walls within the Port of Rotterdam, the authors learned that it is important to verify the accuracy of the monitoring system's measurements before dredging the quay wall. This helps to better understand whether any anomalous measurement results are caused by (unexpected) physical phenomena or by errors in the monitoring system. This preliminary verification ('Site Acceptance Test', abbreviated as 'SAT') was carried out for all instrumented tubular piles and ground anchors. No SAT was performed for the driven cast-in-situ piles, as this would be difficult to implement and very costly.

3.1 *Tubular piles*

The tubular pile is measured while lying down in a hall, free from meteorological effects such as sunlight and temperature, or other influences that could cause a local increase in the temperature/strain of the steel of the tubular pile.

For each instrumented tubular pile, a 3-point bending test is performed to verify whether the measured strains are consistent with the theoretically expected values. For this, the tubular pile

is supported at its ends, and loaded halfway along the span using 2 hydraulic jacks (Figure 4). The force exerted by the jacks in this test setup corresponds to a steel stress of 100 MPa in the outermost fiber of the tubular pile (i.e., at the location of the fiber optic sensor lines). The jack force is increased in steps of 20% of the maximum force. At each step, strain measurements are performed.

Figure 4. Photo of the 3-point bending test

At the time of performing the 3-point bending test, only the two glued fiber optic sensor lines are present on each tubular pile. A combined strain and temperature fiber optic cable (DTSS) was used. The advantage of this cable is that the strain and temperature fibers are located within the same cable, which makes it easier to install.

The temperature cable should normally be decoupled ('loose-tube') such that it only responds to temperature changes and not to mechanical strain. However, Figure 5 shows that during the execution of the 3-point bending test, mechanical strains developed in the temperature fiber. The maximum mechanical strain in the temperature fiber was approximately 10% of the maximum strain in the strain fiber. Based on a thermal coefficient of 7.32 * 10^{-6}/°C for fiber optics and 12 * 10^{-6}/°C for steel, temperature compensation would then result in an error of 19.32/7.32 × 10% = approximately 25% of the maximum mechanical strain. Since such an error is unacceptably large, it was decided - based on these test results - to use a different type of temperature cable in an oversized tube for the fiber optic sensors which are installed by grouting after pile driving. This clearly demonstrates the added value of performing a Site Acceptance Test. The explanation for this phenomenon may be found in the lateral deformations caused by bending, which lead to friction in the loose-tube temperature fiber. Since bending is less dominant in the driven cast-in-situ piles, no oversized tube has been applied there.

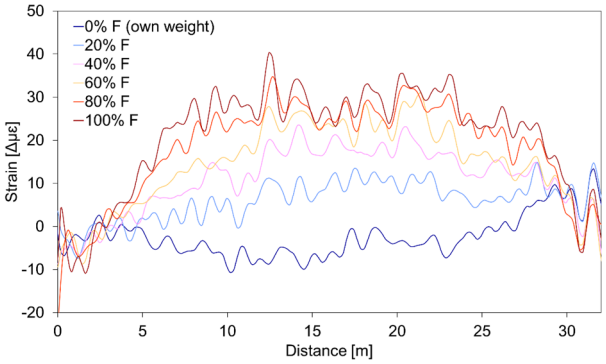

Figure 5. Strain of the temperature fiber during the 3-point bending test versus distance. The distance is measured along the pile axis.

For each load step, the strains and deformations were predicted using SCIA Engineer software. Figure 6 shows a good agreement between the measurements and the predictions, validating the accuracy of the strain measurements. Only in the load transfer zone around the hydraulic jacks does the predicted strain overestimate the actual strain. Since this is a local effect, it is not relevant to the dredging situation, where the tubular pile is subjected to rather uniform loads. In Figure 7, the vertical deformations (measured with a total station) are compared with the predicted deformations. These match well, allowing the conclusion that the actual bending stiffness of the tubular pile corresponds closely to the assumed theoretical value.

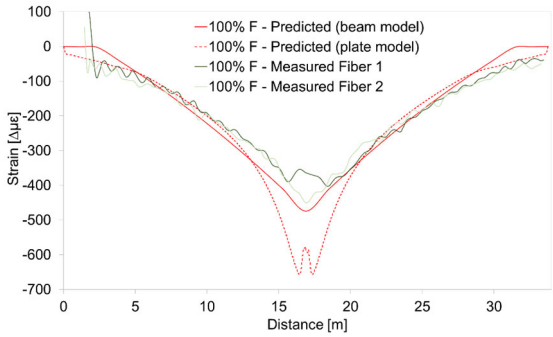

Figure 6. Measured strain versus predicted strain at 100% load.

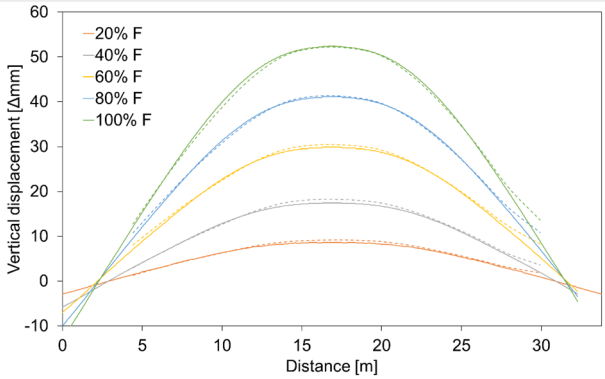

Figure 7. Vertical displacement of the tubular pile during the 3-point bending test. The dashed line represents the measured values, and the solid line shows the predictions made using a plate model.

3.2 *Ground anchors*

For ground anchors, it is common practice to perform an acceptance test or suitability test to verify the geotechnical load-bearing capacity. This also presents an excellent opportunity to carry out a Site Acceptance Test. During the execution of the acceptance or suitability test, fiber optic strain measurements are performed. It can then easily be verified whether the measured force corresponds to the force applied by the hydraulic jack.

In the first analysis, strains were converted to stresses using a fixed E-modulus of ca. 210 GPa for hollow anchor rods, as is common practice. This resulted in calculated anchor forces significantly exceeding the force applied by the hydraulic jack, which is physically impossible. The explanation for this observation was found in the results of the Limellete anchor load testing campaign in Belgium (BBRI, 2008), where significant non-linear stress-strain behavior of hollow anchor rods was reported. The steel grade E470 does not show a clear yield point. The yield stress is defined as the stress at which the steel exhibits a permanent (plastic) strain of 0.2%. Consequently, during anchor testing, significant plastic deformations are observed.

The tangent stiffness of the anchor rods was derived using the Fellenius method (Fellenius, 2001). In Figure 8, the same method is applied to analyze the Amaliahaven strain measurements. A strain-dependent modulus of elasticity is derived for the hollow anchor rods (green trend line). Without the Site Acceptance Test, it would likely be very difficult to interpret the measurement results later in the project, as the use of a fixed E-modulus of ca. 210 GPa would introduce a significant error in the conversion from strain to stress.

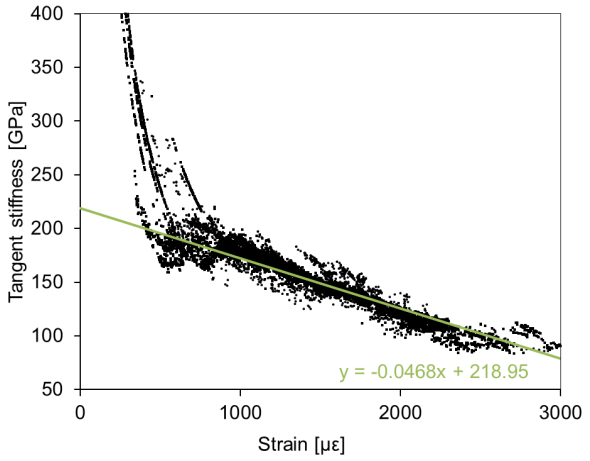

Figure 8. Strain-stiffness behavior of anchor rods from Fellenius method.

Figure 9 now shows that the measured force closely matches the applied force in load steps 4 and 5. The same figure also shows that the anchor force remains constant over the first 25 meters of the anchor, which corresponds to the free length of the anchor. From 25 meters onward, the anchor force decreases with length, indicating the presence of the grout body.

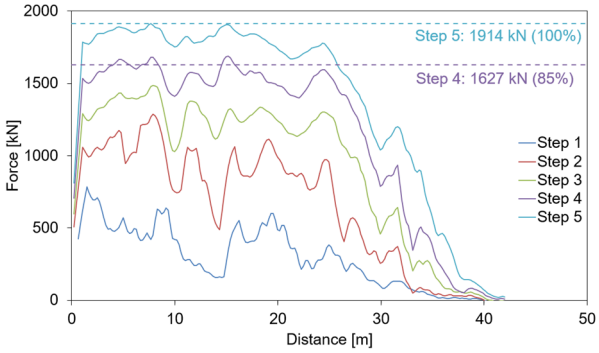

Figure 9. Measured (solid line) versus applied (dashed line) anchor force. The distance is measured along the axis of the anchor.

4 DATA ANALYSIS

The total set of monitoring as described in Chapter 2 provides a vast amount of data, which must be visualized and made understandable at the same time. In general, the data analysis can be approached from two different perspectives. First, a qualitative view is given upon the data where the behaviour of the quay wall is related to certain events like the dredging process. Secondly, a more in-depth quantitative view is given upon the data where the desired physical quantities (see §2.2.1) can be compared to the Plaxis2D models.

4.1 *Qualitative perspective*

Within the qualitative perspective, the data is converted up until mechanical strains, corresponding to step 2 from §2.1. In this way, a compromise is found between 'physically meaningful data' and an 'efficient analysis'. An example is shown for the fiber optic sensors of the tubular piles. The data is directly compared to the dredging phases, since this is the dominant load on the quay wall. Furthermore, the inclinometer measurements of the tubular pile are shown and related to the dredging process.

4.1.1 *Tubular piles – Fiber optic sensors*

A color intensity plot shows the mechanical strains in all four fiber optic sensors of a tubular pile (Figure 10). The location of these sensors within the cross-section (15°/165°/195°/345°) is shown in Figure 2. Accordingly, three dimensions are made visible in Figure 10; the depth/length of the pile, the time aspect and the magnitude of the mechanical strain. Indicatively, the dredging depth in front of the quay wall is included as well, expressed to the reference level NAP.

A very clear correlation between mechanical strain and dredging depth becomes visible for the tubular pile, which implies that bending moments develop directly during the dredging phase. Note that a bending moment becomes visible once the mechanical strains between the water- and landside differ significantly, see Figure 10. Another conclusion that can be drawn is that the glued fiber optic sensors (15° and 195° cfr. Figure 2) show the most fluent behavior, whereas the grouted sensors show a more erratic signal (165° and 345° cfr. Figure 2).

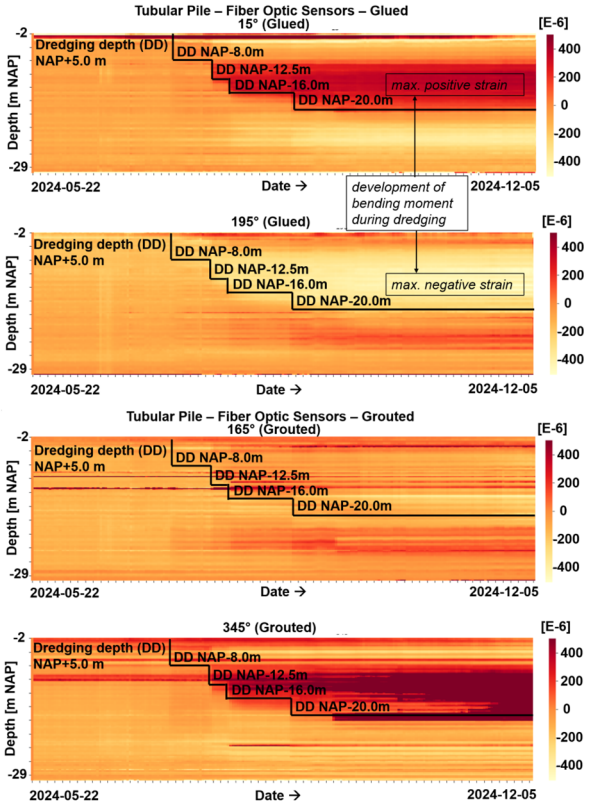

Figure 10. Color intensity plot of mechanical strains - tubular pile.

4.1.2 *Tubular Piles – Inclinometer measurements*

The inclinometer measurements have a 'discontinue character' and are manually performed throughout the different phases of the dredging process. The tubular pile inclinometer casing is extended in the front wall of the relieving platform. In Figure 11, one can find the deformation, projected

perpendicular to the quay wall, during the different dredging phases. The upper 7m in the graph corresponds to the front wall of the relieving platform, the section below corresponds to the tubular pile.

Before dredging and after backfilling, at a level of 'NAP+5.0 m', the tubular pile and relieving platform front wall tilt slightly backward. Once the dredging process starts, with measurements at NAP-5.0 m, NAP-15.0 m and NAP-20.0 m, the deformations strongly develop. Concluding, a clear correlation becomes visible between the development of deformations and the dredging process.

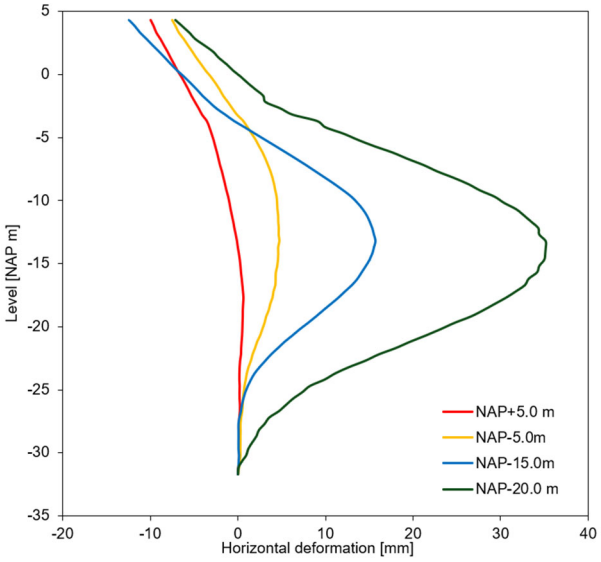

Figure 11. Inclinometer measurements of tubular pile and relieving platform front wall at dredging.

4.2 *Quantitative perspective*

Within the quantitative perspective, a more in-depth analysis is performed in order to assess the validity of the data. The situation with a dredging depth equal to NAP-20.0 m is considered. At this stage, no significant water level difference is present over the combined wall. This boundary condition is substantiated by the data from the present piezometers.

1. Fiber optic sensors

The fiber optic sensor data is translated into physical quantities N and M_y according to §2.1. Only the glued fibers are considered since these sensors provide the best output, as concluded in the qualitative perspective from §4.1.1.

2. Inclinometer measurement

As described in §2.1, the local curvature can be derived from the inclinometer measurement in order to determine the bending moment M_y. Note that a polyfit line is generated through the inclinometer measurement in order to retrieve a fluent bending moment line, as one would expect. In this way, measurement errors are dealt with. Furthermore, the top part of the tubular pile is not considered within the polyfit. The inclinometer measurement reaches all the way through the front wall of the superstructure which has a negligible curvature due to the very stiff concrete. Hence, a polyfit including this upper concrete part would strongly influence the accuracy of the fit, especially at the top of the tubular pile.

The quantitative analysis is finalized by comparing the upper two methods – through fiber optic sensors and inclinometer measurements – to the design model in Plaxis2D. The characteristic values M_{Ek} are shown. See Figure 12.

The first conclusion is that all bending moment curves show a very similar behavior, with a maximum value around NAP-15.0 m. The inclinometer measurement is in good agreement with Plaxis2D in this section of the pile, which makes sense because of the polyfit method. The fiber optic sensors show a better fit at the top of the tubular pile. The fixed end moment at the bottom is also in rather good agreement for all three lines, apart from erratic behavior for the fiber optic sensors. In general, it seems that the Plaxis2D model approximates reality rather well.

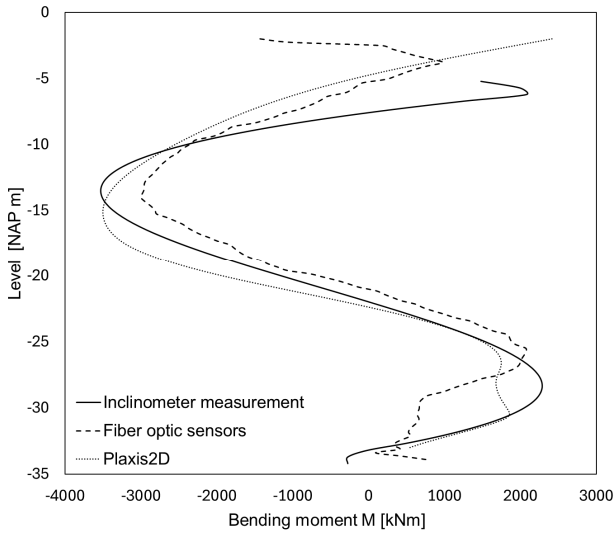

Figure 12. Comparison of bending moments - tubular pile

5 CONCLUSIONS AND FUTURE

This paper presents best practice examples on the monitoring and data analysis of deep-sea quay walls in the Amaliahaven in the Port of Rotterdam. For the critical measurement locations, appropriate sensors were selected. During construction, sensors underwent rigorous Site Acceptance Testing to ensure accuracy. The examples in this paper demonstrate that conducting full-scale Site Acceptance Tests is an essential part of collecting reliable monitoring data. A first glimpse at the data shows that the quay wall has a strong response to the dredging process, where bending moments in the tubular piles develop and stabilize post-dredging. Also from a quantitative perspective, the data shows that the order of magnitude of bending moments in the tubular piles coincides well with the Plaxis2D model of the quay wall. This paper shows the potential value of monitoring data for understanding the quay wall's behavior and updating of computational models, as in the coming years a lot of monitoring data will be collected for a range of different boundary conditions, such as tidal effects, temperature and seasonal changes, mooring loads and crane loads.

6 REFERENCES

Fellenius, B.H., 2001. From strain measurements to load in an instrumented pile. *Geotechnical News Magazine* 19, 35-38.

BBRI, 2008. *Proceedings of the international symposium "Ground anchors – Limelette test field results", Volume 1*, Brussels, 5-6.